AIAA 99-0977
Critical Behavior in Small Particle Combustion

Robert S. Hiers III
Sverdrup Technology, Inc., AEDC Group
Arnold Engineering Development Center
Arnold Air Force Base, Tennessee 37389

37th AIAA Aerospace Sciences Meeting & Exhibit
January 11-14, 1999 / Reno, NV

Critical Behavior in Small Particle Combustion*

Robert S. Hiers III†
Sverdrup Technology, Inc., AEDC Group
Arnold Engineering Development Center
Arnold Air Force Base, Tennessee 37389

Abstract

Small particles combusting under free molecular conditions are shown to exhibit critical behavior under conditions of high collision efficiency. At a particular collision efficiency the particle behavior transitions from non-critical to critical (or runaway) behavior. Non-critical behavior is defined as a finite particle temperature at burnout, while critical behavior implies an infinitely increasing particle temperature at burnout. The critical collision efficiency is derived from the governing equations for free molecular combustion of small particles. The critical collision efficiency is shown to be a function of the specific heats of the gas and the particle, and is independent of the particle size. Analytic and numerical results are compared. Particle radiation is included in the numerical results. The inclusion of radiation does not effect the critical collision efficiency, although radiation does decrease the rate of particle temperature increase.

Nomenclature

A	Particle surface area
C	Particle specific heat
C_p	Gas-specific heat at constant pressure
C_v	Gas-specific heat at constant volume
$\hat{C}_V$	Gas-specific heat at constant volume under effusive conditions
D	Particle diameter
E	Particle internal energy
e	Particle specific internal energy
f	Collision efficiency
$h_f^o(0)$	Enthalpy of formation at 0 K
k	Boltzmann constant
k_r	Spectrally averaged emission coefficient
m	Gas molecular mass
$\tilde{m}$	Mass of carbon atoms removed from particle per reactive collision
M_W	Gas molecular weight
n	Gas number density
N_A	Avogadro's number
P_∞	Ambient pressure
q_{nr}	Energy transferred to the particle by a non-reactive collision
q_r	Energy transferred to the particle by a reactive collision
$\Re$	Specific gas constant
r	Particle radius
r_0	Initial particle radius
t	Time
t^*	Particle burnout time
T	Particle temperature
T_0	Reference temperature or initial particle temperature
T_∞	Ambient temperature
T^*	Particle burnout temperature
u	Gas thermodynamic internal energy
V	Particle volume
$\bar{v}$	Average molecular velocity
X	Stoichiometric coefficients

* The research reported herein was performed by the Arnold Engineering Development Center (AEDC), Air Force Materiel Command. Work and analysis for this research were performed by personnel of Sverdrup Technology, Inc., AEDC Group, technical services contractor for AEDC. Further reproduction is authorized to satisfy needs of the U. S. Government.

† Senior member, AIAA.

Z	Collision frequency
α	Particle surface thermal accommodation coefficient
γ	Gas ratio of specific heats
ε	Particle emissivity
λ	Gas mean free path
μ	Gas kinematic viscosity
ρ	Particle material density
ρ_∞	Ambient gas density
σ	Stefan-Boltzmann constant
ω	Specific oxidation rate

Introduction

The term "critical behavior" is used to describe many different aspects of combustion, e.g., ignition vs. non-ignition, explosion vs. non-explosion, vigorous vs. weak combustion. In general, criticality indicates an abrupt transition from a stable or well-behaved configuration to a completely different, potentially unstable configuration. The critical combustion behavior of spherical carbon particles has been examined previously by Trevino, Higuera, and Liñan.[1] Additionally, Zhang[2] analyzed bifurcation behavior in a homogeneous-heterogeneous system. In each of these instances, the particle combustion was assumed to occur under continuum conditions. Hiers[3,4] has shown that the combustion of soot particles occurs under substantially rarefied or free molecular conditions for most practical applications. The objective of this paper is to identify a regime of critical behavior for particles combusting under free molecular conditions – indicated by an infinitely increasing particle temperature at burnout.

Free Molecular Combustion Model

Complete details of the free molecular combustion model are given in Refs. 3 and 4. A brief derivation is given here. Each term is defined in the Nomenclature above. All thermal properties of the particle and the surrounding gas are assumed to be temperature-dependent in this derivation. Additionally, the particle is treated as a lumped, one-dimensional spherical system. If we denote the particle thermal energy as E, then E is given by

$$E = \rho V(t) e(T) \tag{1}$$

where ρ is the material density (assumed constant), V is the particle volume, and e is the particle-specific internal energy (energy per unit mass). Since particle volume is simply $4/3\pi r^3$, then E is a function of both particle radius, r, and particle temperature, T. Since both V and T (and thus e) are functions of time, then the rate of change of E is

$$\frac{dE}{dt} = \frac{\partial E}{\partial e}\frac{de}{dt} + \frac{\partial E}{\partial V}\frac{dV}{dt} \tag{2}$$

The partial derivatives are obviously

$$\frac{\partial E}{\partial e} = \rho V \tag{3}$$

and

$$\frac{\partial E}{\partial V} = \rho e \tag{4}$$

since we are treating the particle material density as a constant. Additionally, we can apply the chain rule to yield

$$\frac{dV}{dt} = \frac{\partial V}{\partial r}\frac{dr}{\partial t} \tag{5}$$

where

$$\frac{\partial V}{\partial r} = \frac{\partial}{\partial r}\left(\frac{4}{3}\pi r^3\right) = 4\pi r^2 = A \tag{6}$$

where A is the particle surface area. Making these substitutions into Eq. (2) yields

$$\frac{de}{dt} = \rho V\frac{de}{dt} + \rho e A\frac{dr}{dt} \tag{7}$$

We can write the internal energy as

$$e = \int_{T_0}^{T} C d\hat{T} + e(T_0) \tag{8}$$

where C is the particle specific heat (a function of temperature) and T_0 is some reference temperature. If we use the thermodynamic properties of graphite (a reference element) for soot, then $e(T_0)$ is defined to be zero. Throughout this paper, the reference temperature (T_0) is assumed to be 0 K. Applying Leibnitz's Rule yields

$$\frac{de}{dt} = \frac{d}{dt}\int_{T_0}^{Tt} C(\hat{T})\,d\hat{T}$$

$$= C[T(t)]\frac{d}{dt}T(t) - CT_0\frac{d}{dt}T_0 + \int_{T_0}^{T(t)} \frac{\partial}{\partial t}[C(\hat{T})]\,d\hat{T} \quad (9)$$

but

$$\frac{d}{dt}(T_0) = 0 \quad (10)$$

and

$$\frac{\partial}{\partial t}[C(\hat{T})] = 0 \quad (11)$$

since C is not an explicit function of time. Therefore, Eq. (9) simplifies to

$$\frac{de}{dt} = C\frac{dT}{dt} \quad (12)$$

Substituting Eq. (12) into Eq. (7) yields

$$\frac{dE}{dt} = \rho VC\frac{dT}{dt} + \rho eA\frac{dr}{dt} \quad (13)$$

Furthermore, since

$$V = A\frac{r}{3} \quad (14)$$

then Eq. (13) will simplify to

$$\frac{dE}{dt} = A\left[\rho\frac{r}{3}C\frac{dT}{dt} + \rho e\frac{dr}{dt}\right] \quad (15)$$

If we assume we are given the specific oxidation rate, ω(g/cm^2/sec), as a function of temperature and pressure, we can find the rate of change of the particle radius since

$$-\omega A = \rho\frac{dV}{dt} = \rho A\frac{dr}{dt} \quad (16)$$

or

$$\frac{dr}{dt} = -\frac{\omega}{\rho} \quad (17)$$

Substituting Eq. (17) into Eq. (15) yields

$$\frac{dE}{dt} = A\left[\frac{\rho r}{3}C\frac{dT}{dt} - \omega e\right] \quad (18)$$

This is the rate of change of the energy content of the particle.

The free molecular model is one of collision-counting. A collision which results in an exothermic reaction adds energy to the particle. An endothermic reaction removes energy. Non-reactive collisions will either add or subtract energy from the particle: adding if the gas is hotter than the particle, subtracting if the particle is hotter than the gas. Also, if a reaction occurs, mass must be removed from the particle.

If the characteristic body dimension is small compared to the gas mean free path, the body is in free molecular flow, and heat transfer will occur only by direct collisions with the ambient gas molecules (ignoring radiation for the moment). Upon collision with the particle surface, the gas molecules will exchange energy with the surface, either by transferring thermodynamic internal energy and translational energy, or by chemically reacting with the particle surface. The term "thermal accommodation" refers to the effectiveness of the energy exchange between the gas and the particle during a collision. Perfect thermal accommodation is assumed throughout this work, which means that the energy modes of a gas molecule come to thermal equilibrium at the particle temperature. This is reasonable for low thermal energy collisions with rough surfaces such as those considered here.[5] We can express the oxidation rate (ω) as a fraction of the total number of collisions; i.e.,

$$\omega = Zf\tilde{m} \quad (19)$$

where Z is the total collision frequency, Zf is the frequency of reactive collisions, f is termed the collision efficiency, and $\tilde{m}$ is the mass removed per reactive collision. Assuming no relative motion between the particle and the gas (dynamic equilibrium), the collision rate Z is given by Ref. 6

$$Z = \frac{1}{4}n\bar{v} = \frac{1}{4kT_\infty}P_\infty\sqrt{\frac{8kT_\infty}{\pi m}} \quad (20)$$

where k is Boltzmann's constant, $\bar{v}$ is the average molecular velocity, n is the number density, m is molecular mass, and P_∞ and T_∞ are the pressure and temperature of the ambient gas. The energy flux at the particle surface due to collisions with gas molecules can therefore be given as

$$\frac{dE}{dt}_{collisions} = [Zfq_r + Z(1-f)q_{nr}]A \quad (21)$$

where q_r is the energy transferred to the particle by a reactive collision and q_{nr} is the energy transferred by a non-reactive collision. The internal energy (u) of a gas molecule has contributions from translational energy, internal structure (e.g., vibrational and rotational energy) and chemical potential energy (bond energy). We can write the internal energy of the gas molecules as

$$u = u_{translational} + u_{internal} + u_{chemical} \quad (22)$$

Since the particle is smaller than the mean free path, the molecular flux to the particle surface is effusive. Therefore, the average translational energy of the gas molecules incident on the particle surface is $2kT$.[7] Also, since the reference temperature is chosen as 0 K, the chemical potential energy is simply the enthalpy of formation at 0 K, or $h_f^o(0)$. Therefore, the internal energy of a gas molecular at any temperature T is shown in Ref. 8

$$u(T) = 2kT + \int_0^T C_{v,\,internal}\,d\hat{T} + h_f^o(0) \quad (23)$$

The change in the internal energy during a single gas-surface collision is given by

$$\Delta u = u_{products} - u_{reactants} \quad (24)$$

or, using Eq. (25),

$$\Delta u = \sum_{i\,products} X_i \left(2kT_i + \int_0^{T_i} C_{v,\,internal}\,d\hat{T} + h_f^o(0) \right) - \sum_{j\,reactants} X_j \left(2kT_j + \int_0^{T_j} C_{v,\,internal}\,d\hat{T} + h_f^o(0) \right) \quad (25)$$

where X denotes the stoichiometric coefficients of the reaction under consideration. Equation (25) can be used to find the change in internal energy for either reactive or non-reactive collisions. By the First Law of Thermodynamics, the energy transferred to the particle during the collision is simply the negative of the change in internal energy of the collision. Therefore, for a non-reactive collision

$$q_{nr} = -\Delta u_{nr} \quad (26)$$

and for a reactive collision

$$q_r = -\Delta u_r \quad (27)$$

The JANAF Thermochemical Tables[9] and associated curve fits[10] are used for all specific heats and heats of formation appearing in Eq. (25).

Equation (21) represents the flux of energy at the particle surface due to collisions with ambient gas molecules. The particle will also exchange energy with the environment by radiation. The rate of radiant energy transfer is given by

$$\frac{dE}{dt}_{radiation} = \varepsilon\sigma\left(T_\infty^4 - T^4\right)A \quad (28)$$

where σ is the Stefan-Boltzmann constant. The treatment of small particle radiation is explained in more detail in Appendix D of Ref. 3. Briefly, small particles are mass (or volume) radiators.[11] The emissivity (ε) is thus directly proportional to the particle radius. Therefore,

$$\frac{dE}{dt}_{radiation} = rk_r\sigma\left(T_\infty^4 - T^4\right)A \quad (29)$$

where k_r (the spectrally averaged emission coefficient) is a function of particle temperature, and is derived from the Lee and Tien[12] soot optical properties. The total energy flux at the particle surface is therefore the sum of Eqs. (21) and (28), or

$$\frac{dE}{dt}_{fluxes} = [Zfq_r + Z(1-f)q_{nr}]A + rk_r\sigma\left(T_\infty^4 - T^4\right)A \quad (30)$$

Substituting Eq. (19) into Eq. (18) yields

$$\frac{dE}{dt}_{fluxes} = A\left[\frac{\rho r}{3}C\frac{dT}{dt} - Zf\tilde{m}e\right] \quad (31)$$

Equating Eqs. (30) and (31) and solving for the rate of change of temperature yields

$$\frac{dT}{dt} = \frac{3Z}{\rho rC}[f(\tilde{m}e + q_r) + (1-f)q_{nr}] + \frac{3k_r\sigma}{\rho C}\left(T_\infty^4 - T^4\right) \quad (32)$$

Note that the particle radius, r, appears in Eq. (32) as an unknown function of time. However, substituting Eq. (19) into Eq. (17) yields an ordinary differential equation for the particle radius

$$\frac{dr}{dt} = \frac{-Zf\tilde{m}}{\rho} \tag{33}$$

Since f is also a function of particle temperature, Eqs. (32) and (33) form a coupled set of nonlinear ordinary differential equations for the particle temperature and radius as functions of time. These equations are statements of energy conservation and mass conservation, respectively. In later sections these equations will be integrated in time using a modified implicit Euler method described in Appendix E of Ref. 3.

Critical Combustion Behavior Analysis

Equations (32) and (33) comprise a first-order, nonlinear set of ordinary differential equations for the particle radius and temperature as functions of time. The nonlinearity is due both to the radiation term (T^4) and the nonlinear dependence of the various coefficients (collision efficiency, specific heat, etc.) on the particle temperature. The equations can be linearized by neglecting radiation and assuming that all thermal properties are constant. If the thermal properties are assumed constant, then

$$e = CT \tag{34}$$

and

$$q_{nr} = (2k + C_{\dot{v}internal})(T_\infty - T) = \hat{C}_V(T_\infty - T) \tag{35}$$

from which the definition of $\hat{C}_V$ (the gas-specific heat at constant volume under effusive conditions) is obvious. Making these substitutions in Eq. (32), and neglecting radiation, yields

$$\frac{dT}{dt} = \frac{3Z}{\rho rC}[f(\tilde{m}CT + q_r) + (1-f)\hat{C}_V(T_\infty - T)] \tag{36}$$

For constant collision efficiency, the particle mass equation [Eq. (33)] will integrate immediately to yield

$$r(t) = r_0 - \frac{Zf\tilde{m}}{\rho}t \tag{37}$$

where r_0 is the initial particle radius. Equation (36) is a linear, first-order, ordinary differential equation with variable coefficients (since $r = r(t)$) which can be simply integrated using an integrating factor to obtain

$$T(t) = -\beta + (T_0 + \beta)\left(\frac{r_0}{r(t)}\right)^{\delta} \tag{38}$$

where

$$\beta = \frac{[fq_r + (1-f)\hat{C}_V T_\infty]}{[f\tilde{m}C - (1-f)\hat{C}_V]} \tag{39}$$

and

$$\delta = 3\left[1 - \frac{(1-f)\hat{C}_V}{f\tilde{m}C}\right] \tag{40}$$

and T_0 is the initial particle temperature.

This analytic solution was used to validate the numerical method. For these calculations, the constant coefficients are evaluated at the following conditions: pure molecular oxygen at a pressure of 0.10 atm, temperature of 2500 K, using oxidation rates from Roth, et al.[13] Figure 1 presents a comparison of the analytical solution and the numerical solution [solving Eqs. (32) and (33)] using the modified implicit Euler scheme described in Appendix E of Ref. 3 for the temperature rise of particles of various size oxidizing under the conditions given above. The numerical solution has been altered to neglect radiation and to use the same constant properties as the analytic solution.

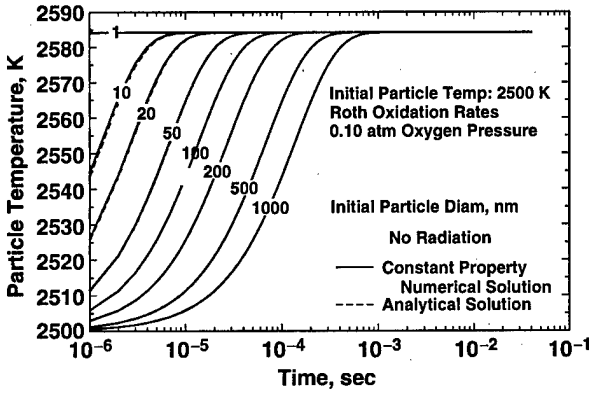

Fig. 1. Comparison of analytical and numerical solutions for particle temperature history.

The analytical and numerical solutions are virtually indistinguishable from each other, except at the smaller particle sizes. The numerical solutions were performed with a constant (10^{-7} sec) step size, which was not small enough to capture the fast rise for the smallest particles. This result validates the bulk of the numerical solution. The only potential errors are in the evaluation of the non-

constant properties and in the treatment of the radiation term. Note in Fig. 1 that the ultimate temperature of the particle is independent of the initial particle size. The initial particle size affects only the rise time.

Including the radiative term in Eq. (36) yields

$$\frac{dT}{dt} = \frac{3Z}{\rho r C}[f(\tilde{m}CT + q_r) + (1-f)\hat{C}_V(T_\infty - T)] + \frac{3k_r\sigma}{\rho C}\left(T_\infty^4 - T^4\right) \quad (41)$$

where k_r is now treated as a temperature-independent constant. Figure 2 presents the same numerical results as Fig. 1, with the addition of the results from the numerical solution, including radiation. The analytical solutions have been removed for clarity. Note that neither the ultimate particle temperature nor the particle lifetime change with the inclusion of the radiation term. Inclusion of the radiation term only increases the time required to reach the ultimate temperature.

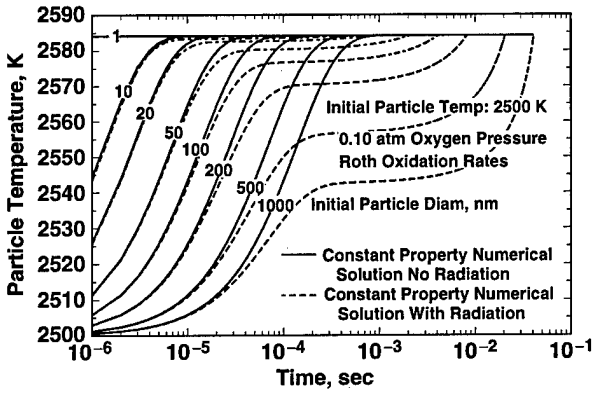

Fig. 2. Comparison of constant property numerical solutions with and without radiation.

Critical Behavior Analysis

The presence of the r_0/r term in Eq. (38) indicates a singularity at burnout (i.e., at $r = 0$). The burnout temperature T^* is the particle temperature as this singularity is approached. The time at which the singularity is reached ($t=t^*$) can be found by setting $r(t) = 0$ in Eq. (37):

$$t^* = \frac{r_0\rho}{Zf\tilde{m}} \quad (42)$$

and so we can define

$$T^* = \lim_{t\to t^*}[T(t)] \quad (43)$$

The burnout temperature (T^*) exhibits two distinct behaviors depending upon the value of the exponent δ:

$$\delta < 0 \Rightarrow T^* \to -\beta \quad (44)$$

$$\delta \geq 0 \Rightarrow T^* \to \infty \quad (45)$$

Allowing the collision efficiency (f) to vary while considering all other parameters fixed, we can solve Eq. (40) for the critical value of $f = f^*$ that corresponds to $\delta = 0$. This yields

$$f^* = \frac{1}{1 + \frac{\tilde{m}C}{\hat{C}_V}} \quad (46)$$

which for the numerical values of the other parameters yields $f^* = 0.401$. This means

$$f < f^* \Rightarrow \delta < 0 \Rightarrow T^* \to -\beta \quad (47)$$

$$f \geq f^* \Rightarrow \delta \geq 0 \Rightarrow T^* \to \infty \quad (48)$$

Physically, the collision efficiency f must be between 0 and 1. Therefore, both behaviors are possible, and a bifurcation exists at $f = f^*$. Results from Eq. (38) are plotted in Fig. 3 for various values of the collision efficiency f. The computations stop one time step before burnout to avoid the infinite temperature at the singularity.

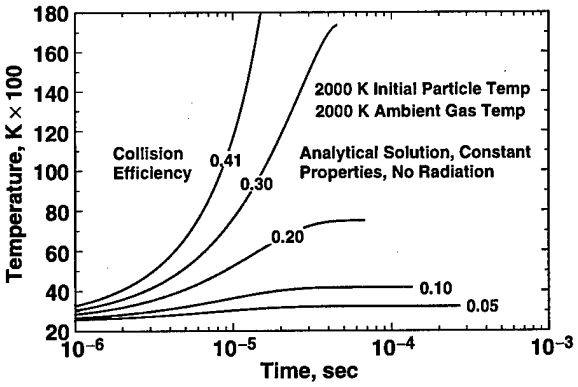

Fig. 3. Analytical solution for temperature history as a function of collision efficiency.

Note the change in the behavior of the slope of the temperature-time history as f becomes larger than f^*. The slope at burnout changes from practically zero to very large as the collision efficiency increases. Figure 4 is a re-scaled version of Fig. 3 to show the complete curve at $f = 0.41$. The "small f" behavior would be typical under most physical conditions. The "large f" behavior would be approached only under the conditions of very efficient reactive collisions (such as with atomic oxygen) and no nonreactive gases (such as nitrogen). These conditions are not typically found in flames, shock tubes, or other practical combustion devices. However, these conditions may be encountered in the combustion of ablative materials (such as carbon) in atmospheric reentry.

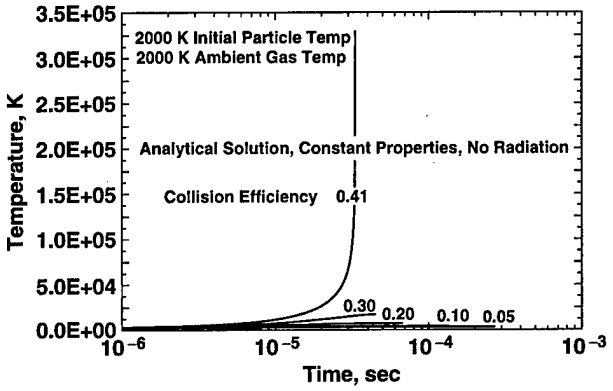

Fig. 4. Analytical solution for temperature history as a function of collision efficiency - rescaled.

The large temperatures indicated are not physical, since other processes that are ignored here would become important. Two such processes are thermal vaporization (which will continue to be ignored) and radiation. Radiation will now be considered.

Equation (41) is the particle energy equation including radiative loss. Figure 5 shows the numerical solution of Eq. (41) for particle temperature versus time. The collision efficiency (f) is varied while considering all other parameters fixed.

The "small f" and "large f" behaviors noted in Fig. 3 are also seen when including radiative heat loss. Figure 6 is a rescaled version of Figure 5 to show the complete curve for $f = 0.41$. Note that the addition of the radiative term did not change the ultimate particle temperature. Once again, the high

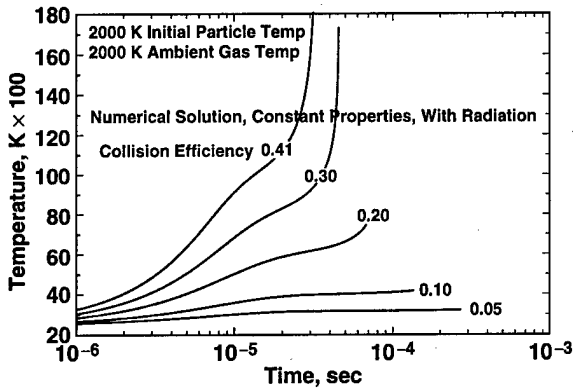

Fig. 5. Numerical solution for temperature history as a function of collision efficiency (with radiation).

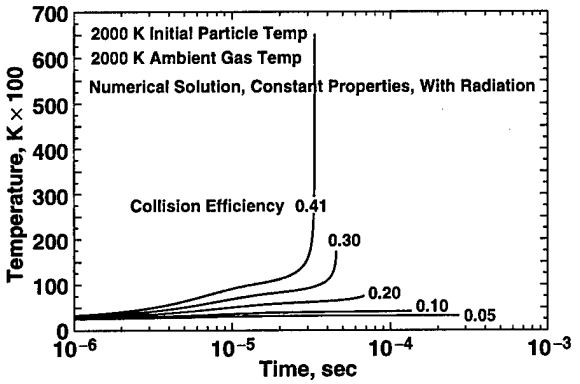

Fig. 6. Numerical solution for temperature history as a function of collision efficiency (with radiation) - rescaled.

temperatures indicated here are not physical, since thermal vaporization will become important at about 4000 K. This mechanism would remove mass (and thus energy) from the particle while holding the particle temperature down. As in the previous figures, the calculations are stopped one time step before burnout to avoid the singularity which occurs when the particle radius is reduced to zero.

Figure 7 shows the solutions for both the analytical solution without radiation and the numerical solution with radiation. For small collision efficiencies, the curves are practically indistinguishable, but the radiation term does increase the temperature rise time, as noted in the previous section. For larger values of the collision efficiency, the slope of the temperature at burnout is practically zero for the no-radiation cases, but is very large for the cases considering radiation. The inclusion of radia-

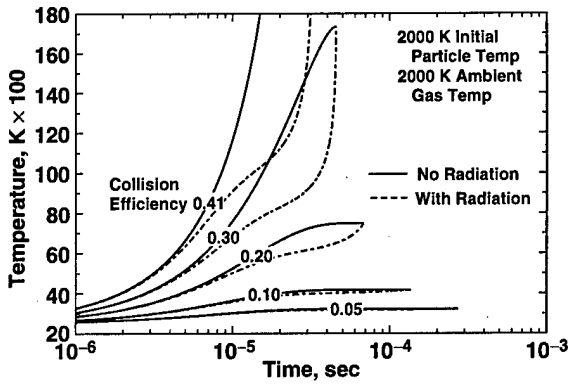

Fig. 7. Comparison of analytical and numerical (with radiation) solution for temperature history as a function of collision efficiency.

tion reduces the value of the collision efficiency required to produce a large slope at burnout. The critical value for infinite temperature at burnout is unaffected by the inclusion of radiation.

Summary/Conclusions

A bifurcation is seen in the behavior of small particles combusting under free molecular conditions. For relatively low collision efficiencies (or kinetic rates), the particle temperature is bounded as the particle size reduces to zero at burnout. As the collision efficiency is increased, the particle temperature at burnout increases, but still remains bounded. At some critical value of collision efficiency, the particle temperature at burnout is unbounded, and increases without limit. Under the assumption of constant thermal properties of both the particle and the surrounding gas, this critical value of the collision efficiency is seen to be a simple function of the gas and particle specific heats and the amount of mass removed per collision. Calculations were presented neglecting and including the effect of particle radiation. The inclusion of radiation increases the time required to reach any given particle temperature, but does not substantially change the critical behavior; i.e., the particle temperature at burnout becomes unbounded at the same critical value of collision efficiency, whether radiation is included or neglected.

The impact of this critical behavior will be important in situations involving high collision efficiency—i.e. high particle temperatures in extremely oxidizing conditions. For instance, the use of laser induced incandescence as a soot diagnostic is typically applied in reducing or at most weakly oxidizing conditions. The kinetic time scales are long enough that reactions on the particle surface during the laser pulse and subsequent particle cooldown are typically ignored. If soot (or other small combustible particles) were present in an oxidizing atmosphere (e.g. ablation or intentional particle injection into the boundary layer of a re-entry vehicle) and laser induced incandescence used as a particle concentration diagnostic, the potential for critical vs. non-critical combustion behavior would have to be assessed.

For the carbon particles considered here, thermal vaporization (sublimation) is expected to have a major impact on the critical behavior as the particle temperatures approach the vaporization temperature of about 4000 K. Particle vaporization will be added to the model in the near future.

References

1. Trevino, C., Higuera, F., and Liñan, "Critical Conditions for Carbon Combustion," *Twenty-First Symposium (International) on Combustion*, The Combustion Institute, 1986, pp. 211-219.

2. Zhang, Dong-Ke, "Bifurcation Behavior in a Homogeneous-Heterogeneous Reaction System with a Constant Power Source," *Combustion and Flame*, Vol. 96, 1994, pp. 171-178.

3. Hiers, R. S., "Rarefaction Effects in Small Particle Combustion," Ph.D. Dissertation, University of Tennessee, August 1997.

4. Hiers, R. S., "Rarefaction Effects in Small Particle Combustion," *AIAA Journal of Thermophysics and Heat Transfer*, Vol.11, No. 2, April-June 1997, pp. 232-238.

5. Schaaf, S. A. and Chambre', P. L., *Flow of Rarefied Gases*, Princeton University Press, Princeton, 1961, pp. 3-11.

6. Kennard, E. H., *Kinetic Theory of Gases*, McGraw-Hill, New York, 1938, pp. 176-180.

7. Oppenheim, A. K., "Generalized Theory of Convective Heat Transfer in a Free-Molecule

Flow," *Journal of the Aeronautical Sciences*, Vol. 20, No. 1, January 1953.

8. Vincenti, W. G. and Kruger, C. H., *Introduction to Physical Gas Dynamics*, Krieger Publishing Co., New York, 1965, pp. 120-139.

9. Chase, M. W., Jr., Davies, C. A. Downey, J. R., Jr., Frurip, D. J., McDonald, R. A., and Syverud, A. N., *JANAF Thermochemical Tables*, Vols. 1-2, 3rd Edition; see also *Journal of Physical and Chemical Reference Data*, Vol. 14, 1985, Supplement 1, American Inst. of Physics, New York, 1986.

10. Gordon, S. and McBride, B. J., "Computer Program for the Calculation of Complex Chemical Equilibrium Compositions, Rocket Performance, Incident and Reflected Shocks, and Chapman-Jouget Detonations," NASA SP-273 and Supplements, March 1976.

11. Kokhanovsky, A. A. and Zege, E. P., "Optical Properties of Aerosol Particles: A Review of Approximate Analytical Solutions," *Journal of Aerosol Science*, Vol. 28, No. 1, 1997, pp. 1-21.

12. Lee, S. C. and Tien, C. L., "Optical Constants of Soot in Hydrocarbon Flames," *Eighteenth Symposium (International) on Combustion*, The Combustion Institute, 1981, pp. 1159-1166.

13. Roth, P., Brandt, O., and Gersum, S. von, "High Temperature Oxidation of Suspended Soot Particles Verified by CO and CO_2 Measurements," *Twenty-Third Symposium (International) on Combustion*, The Combustion Institute, 1990, pp. 1485-1491.